Book Title: ZigBee Network Protocols and Applications

Editors: Chonggang Wang, Tao Jiang and Qian Zhang

September 9, 2009

Contents

Chapter 1

Performance Analysis of the IEEE 802.15.4 MAC Layer

M.R. Palattella, A. Faridi, G. Boggia, P. Camarda, L.A. Grieco, M. Dohler, A. Lozano

In this chapter, the IEEE 802.15.4 MAC layer is modeled using a per-node Markov chain model. Using this model, expressions for various performance metrics including delay, throughput, power consumption, and efficiency, are derived and such expressions are subsequently validated against the corresponding values obtained via simulation. The simplifying assumptions required by the Markov-chain analysis are studied and their impact on the performance metrics is quantified.

1.1 Introduction

As already alluded to in previous chapters of this book, ZigBee is arguably the most prominent alliance dedicated to low-power embedded systems. It is a facilitator of applications pertaining to home and building automation, smart metering, health care, among many others. Its link and access protocols rely on the specifications of IEEE 802.15.4 [1], whereas higher layers are subject to the profile definition of the ZigBee special interest group (SIG). The internet engineering task force (IETF), however, has lately commenced standardizing networking protocols within their 6LoWPAN [2] and ROLL [3] which are assuming IEEE 802.15.4 link layer technology; ZigBee may thus adopt IETFs networking solution in the future. In short, ZigBee is gaining in importance and the underlying IEEE standard ensures that technology is available from multiple vendors.

On the downside, true deployment success stories are fairly rare still which might be due to the fact that it operates in the highly interfered 2.4 GHz ISM band. Also, Zigbee is not alone and needs to compete with Wibree, a low-power solution based on Bluetooth; Wavenis, the only ultra low-power solution on the smart metering market today; Zwave, a short range solution backed by Intel and Cisco; IO-Homecontrol, an international alliance of worldwide leaders for building management solutions; Konnex/KNX, a European standard for home & building automation; Wireless HART, a SIG offering a interoperable wireless communication standards for process measurement and control applications; just to mention a few.

The physical (PHY) layer, which is responsible for maintaining a reliable point-to-point link, is comprised of at least six different solutions. As such, the 2006 revision of the IEEE 802.15.4 standard defines four PHY layers:

- 868/915 MHz Direct Sequence Spread Spectrum (DSSS) with binary phase shift keying;
- 868/915 MHz DSSS with offset quadrature phase shift keying;
- 2450 MHz DSSS with offset quadrature phase shift keying;
- 868/915 MHz Parallel Sequence Spread Spectrum (PSSS), a combination of binary keying and amplitude shift keying.

The 2007 IEEE 802.15.4a version includes two additional PHY layers:

- 2450 MHz Chirp Spread Spectrum (CSS);
- Direct Sequence Ultra-Wideband (UWB) below 1 GHz, or within 3–5 or 6–10 GHz.

Beyond these PHYs at the three bands, there are IEEE 802.15.4c for the 314–316, 430–434 and 779–787 MHz bands in China and IEEE 802.15.4d for the 950–956 MHz band in Japan since these countries recognized that interference in the congested ISM bands is severely deteriorating performance. The above PHY solutions trade complexity with performance and energy efficiency but are all generally facilitating embedded operations at low power.

The medium access control (MAC) layer, which is responsible for maintaining a collision-free schedule among neighbors, is tailored to the low-power needs of embedded radios. There are generally two channel access methods, i.e., the non-beacon mode for low traffic and the beacon-enabled mode for medium and high traffic. The former is a traditional multiple access approach used in simple peer networks; it uses standard carrier sensing multiple access (CSMA) for conflict resolution and positive acknowledgments for successfully received packets. The latter is a flexible approach able to mimic the behavior of a large set of previously published wireless sensor network (WSN) MACs, such as framed MACs, contention-based MACs with common active periods, sampling protocols with low duty cycles, and hybrids thereof [4]; it follows a flexible superframe structure where the network coordinator transmits beacons at predetermined intervals. It successfully combats the main sources of energy drainage by minimizing idle listening, overhearing, collisions and protocol overheads — it may not be the optimum MAC for all applications but covers a large number of envisaged ZigBee applications sufficiently well.

The device classes that are supported by ZigBee are the full function device (FFD), which can be a simple node as well as a network coordinator, and the reduced function device (RFD), which cannot become a network coordinator and hence only talks to a network coordinator. A combination of FDD and RFD allows one to realize any networking topology, such as star, ring, mesh, etc.

Henceforth, we will assume that PHY and networking protocols are given. We will thus

concentrate on formalizing the MAC behavior of IEEE 802.15.4 since it is a crucial step in a successful system deployment with multiple parties suffering from contention. In this chapter, we will only focus on the slotted CSMA/CA mechanism in the beacon-enabled mode. The center of our investigations is to understand the parameters and system assumptions of said MAC and to analyze its performance in terms of delay, throughput, power consumption and efficiency. With these tools at hand, a synthesis of parameters which optimizes a given metric, such as efficiency, becomes feasible. Such a synthesis, even though not explicitly conducted here for space reasons, is central to system designers as it allows one to use derived formulas to optimize the performance of the ZigBee network under given operating conditions. For instance, one could derive analytical expression for a suitable number of contenting nodes to satisfy some trade-off between delay and energy efficiency. Such expressions are currently not available as the synthesis, i.e., inversion of equations characterizing performance, has been deemed too complex. This leaves a field engineer no other choice but to parameterize the rolled-out ZigBee network manually based on a visual inspection of performance graphs. The below outlined approach is hence a significant step forward in that such parametrization can henceforth be automated.

This chapter is structured as follows. In the following section, we will detail the IEEE 802.15.4 MAC structure and its key parameters. We will then review pror works that characterized the performance of said MAC, using a Markov chain model. We then move on to the characterization and analysis of the ZigBee MAC. Finally, conclusions are drawn and future research indications given.

1.2 IEEE 802.15.4 WPANs: an Overview

An IEEE 802.15.4 network [1], known also as Low Rate Wireless Personal Area Network (LR-WPAN), is composed of two different types of devices: FFDs and RFDs. An FFD can operate in three distinct modes serving as: a personal area network (PAN) coordinator, a coordinator, or a device. An FFD can exchange data with both RFDs and other FFDs, whereas an RFD can communicate only with an FFD. RFDs are usually employed in applications that are

extremely simple, e.g., a light switch or a passive infrared sensor, where a very limited amount of data has to be sent to a single FFD. They can be implemented using minimal resources and memory capacity.

In an LR-WPAN, the PAN coordinator (i.e., the central controller) builds the network in its personal operating space. Communications from nodes to coordinator (uplink), from coordinator to nodes (downlink), or from node to node (ad hoc) are possible. Two networking topologies are supported: star and peer-to-peer (Figure 1.1). The star topologies are well suited to PANs covering small areas. In this case, the PAN coordinator controls the communication, acting as a network master. In the peer-to-peer topology, any device can communicate with any other device as long as they are in range of one another. With this kind of topology, more complex networks can be realized (e.g., mesh networks), supporting several types of applications, such as industrial control and monitoring, wireless sensor networks, asset and inventory tracking, and intelligent agriculture. In a peer-to-peer topology, multiple hops can route messages from any device to any other device in the network. A special case of a peer-to-peer network is the cluster tree in which most devices are FFDs. An RFD connects to such a network as a leaf device at the end of a branch because RFDs do not allow other devices to associate. Any of the FFDs can act as a coordinator, providing synchronization services to other devices or other coordinators. Only one of these coordinators can be the overall PAN coordinator, which may have greater computational resources than any other device in the PAN. This requires a mechanism to decide the PAN coordinator and a contention resolution mechanism if two or more FFDs simultaneously attempt to establish themselves as PAN coordinator.

LR-WPANs can operate in two distinct modes: *beacon-enabled* and *nonbeacon-enabled* modes. In the beacon-enabled mode, the time axis is structured as an endless sequence of superframes. Each one comprises an active part and an optional inactive part. The active part is made by a contention access period (CAP), during which a slotted CSMA/CA mechanism is used for channel access, and an optional contention free period (CFP). During the inactive part of the superframe, the devices do not interact with the PAN coordinator and could enter in a low-power state to save energy. In the nonbeacon-enabled mode, the superframe structure is not used, but the unslotted CSMA/CA mechanism is adopted. The

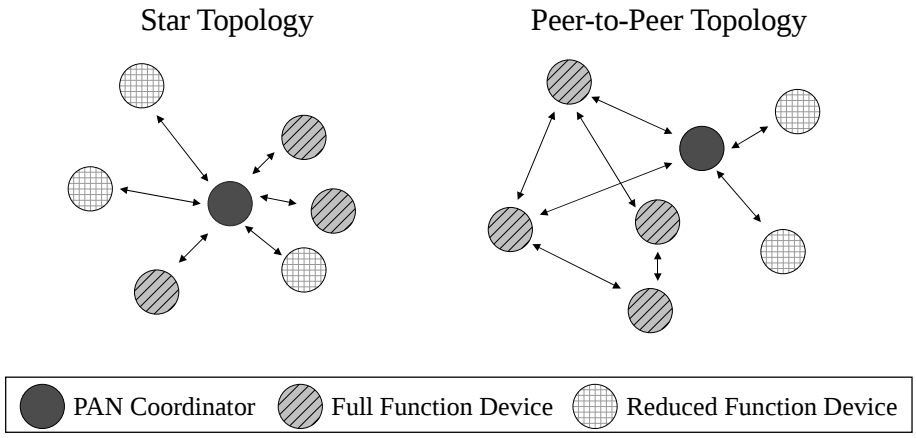

Figure 1.1: Example of IEEE 802.15.4 topologies.

use of beacon-enabled or nonbeacon-enabled modes depends on the application; for example, beacon transmissions are disadvantageous when no periodic or frequent messages are expected from the coordinator, and only sporadic traffic is transmitted by network devices.

It should be noted that the slotted CSMA/CA mechanism adopted with the beacon-enabled mode is different from the well-known IEEE 802.11 CSMA/CA scheme [5]. The main differences are: the time slotted behavior, the backoff algorithm, and the Clear Channel Assessment (CCA) procedure used to sense whether the channel is idle. In the slotted CSMA/CA algorithm, each operation (channel access, backoff count, CCA) can only begin at the boundary of time slots, called backoff periods (BPs). Moreover, unlike in the IEEE 802.11 CSMA/CA scheme, the backoff counter value of a node decreases regardless of the channel status. In fact, only when the backoff counter value reaches zero, the node performs two CCAs, during which it senses the channel to verify if it is idle. This allows a great energy saving compared to IEEE 802.11 CSMA/CA scheme, given that during the listening a significant amount of energy is spent.

1.2.1 Superframe Structure

Herein, more details about the superframe structure adopted in the beacon-enabled mode are given. The format of the superframe is defined by the PAN coordinator. As briefly described before, the superframe consists of an active period and an optional inactive period.

All communications take place in the active period. In the inactive period, instead, nodes are allowed to power down and save energy. Each superframe is bounded by two beacon frames, as shown in Figure 1.2. The beacons are used to synchronize devices attached to the PAN, to identify the PAN, and to give the description of the superframe structure. They are also used for carrying service information for network maintenance, and to notify nodes about pending data in the downlink.

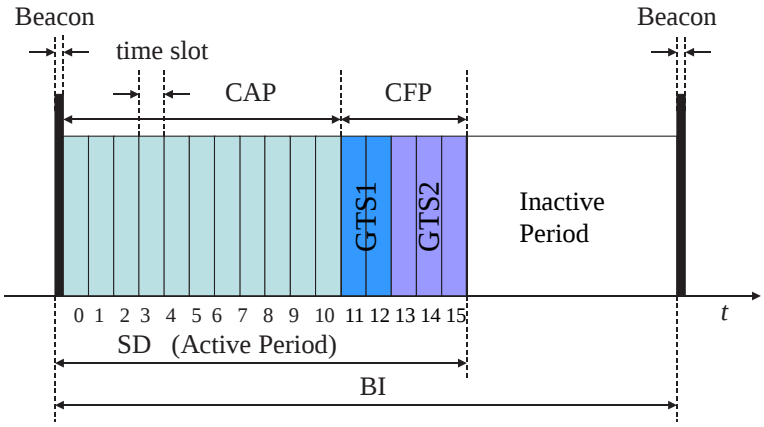

Figure 1.2: MAC superframe.

The length of the superframe, called the Beacon Interval (BI), and the length of its active part, called the Superframe Duration (SD), are determined by the beacon order (BO) and the superframe order (SO) as follows

$$BI = 2^{BO} \times aBaseSuperframeDuration \tag{1.1}$$

$$SD = 2^{SO} \times aBaseSuperframeDuration \tag{1.2}$$

The values of BO and SO are chosen by the coordinator, and have to fulfill the following inequality: $0 \leq SO \leq BO \leq 14$. Instead, the quantity *aBaseSuperframeDuration* denotes the minimum duration of the superframe (corresponding to $SO = 0$) and it is fixed to 960 modulation symbols. Note that in the 2.4 GHz ISM band, a modulation symbol period is equal to 16 μs. We hereafter refer to modulations symbols as simply symbols.

The active portion of a superframe is divided into 16 time slots, each with a duration of $2^{SO} \times aBaseSlotDuration$ symbols, where the constant *aBaseSlotDuration* is equal to 60

symbols. Moreover, as shown in Figure 1.2, the active portion consists of three parts: the beacon, a Contention Access Period (CAP) and a Contention Free Period (CFP). The beacon is sent by the PAN coordinator in the first time slot of the superframe. During the CAP, nodes access the channel using slotted CSMA/CA. The optional CFP is activated upon request from the nodes to the PAN coordinator for allocating guaranteed time slots (GTS). Each GTS consists of some integer multiple of CFP slots and up to 7 GTS are allowed in a CFP.

1.2.2 The Slotted CSMA/CA Mechanism

The basic time unit of the IEEE 802.15.4 MAC protocol is the backoff period (BP), a time slot of length $t_{bp} = aUnitBackoffPeriod = 20$ symbols. In the slotted CSMA/CA algorithm, each operation (channel access, backoff count, CCA) can only start at the beginning of a BP.

Note that a BP is different and smaller than each of the 16 time slots that compose the active period of the superframe shown in Figure 1.2. For example, if $SO = 0$, the superframe slot duration is three times that of a BP. Therefore, a superframe slot duration is always a multiple of three BPs. Moreover, for every node, the first BP boundary in a superframe should be aligned with the first superframe slot boundary of the PAN coordinator.

Each node maintains three variables for each transmission attempt: *NB*, *CW*, and *BE*. *NB* indicates the backoff stage, or equivalently, the number of times the CSMA/CA backoff procedure has been repeated while attempting the current transmission. *CW* is the contention window length, which defines the number of BPs the channel has to be sensed idle before the transmission can start. *BE* is the backoff exponent, which is used to extract the random backoff value. The value of *BE* should fulfill the following inequality: $macMinBE \leq BE \leq macMaxBE$, where *macMinBE* and *macMaxBE* are constants (see Table 1.1).

The slotted CSMA/CA mechanism works as shown in Figure 1.3. Before every new transmission, *NB*, *CW* and *BE* are initialized to 0, 2 and *macMinBE*, respectively. The

node waits for a random number of BPs specified by the backoff value, drawn uniformly in the range $[0, 2^{BE}-1]$. Then, it performs the first CCA, i.e., it senses the channel and verifies whether it is idle. If the channel is idle, the first CCA succeeds and CW is decreased by one. The node then performs the second CCA and, if that is also successful, it can transmit the packet.

If either of the CCAs fail, both NB and BE are incremented by one, ensuring that BE is not more than *macMaxBE*, and CW is reset to 2. The node repeats the procedure for the new backoff stage by drawing a new backoff value, unless the value of NB has become greater than a constant $M = macMaxCSMABackoffs$. In that case, the CSMA/CA algorithm terminates with a *Channel Access Failure* status, and the concerned packet is discarded.

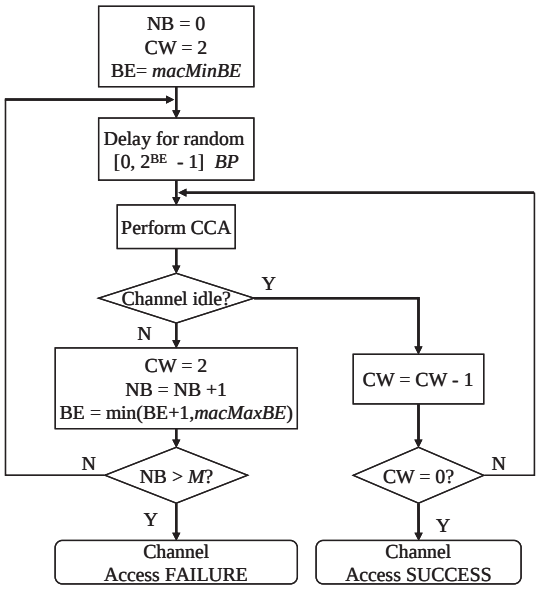

Figure 1.3: Flow chart of the channel access procedure.

A packet transmitted after a successful channel access procedure can be either received successfully or have a collision. The network can be operating in either acknowledged or unacknowledged transmission modes. Hereafter, we refer to these modes as ACK mode and no-ACK mode, respectively.

In ACK mode, a successful transmission is accompanied by the reception of a MAC acknowledgment (ACK), which has a fixed length L_{ack} of 11 bytes (i.e., 22 symbols in the

ISM 2.4 GHz band). The ACK is fed back to the transmitter after a minimum time of $t_{ack}^{-} \leq aTurnaroundTime + t_{bp}$. The constant *aTurnaroundTime* represents time needed for switching the transceiver from one operative mode to another (transmission-to-reception or reception-to-transmission), and has a duration of 12 symbols. The ACK is expected by the sender node to be received before a maximum time t_{ack}^{+} (i.e., the *macAckWaitDuration*), that is equal to $t_{ack/max}^{-} + L_{ack}$ (i.e., 54 symbols). After this time, if the ACK frame is not correctly received, a collision is declared. In this case, the packet is retransmitted using a new transmission procedure with *NB*, *CW*, and *BE* set to their initial values. A packet can be retransmitted at most $R = aMaxFrameRetries$ times if required, before being discarded. The default values of the parameters used in the slotted CSMA/CA procedure, as indicated by the standard [1], are given in Table 1.1.

Table 1.1: Values of slotted CSMA/CA parameters

Parameter	Range	Default Value
macMinBE	0 - 3	3
macMaxBE	/	5
macMaxCSMABackoffs	0 - 5	4
aMaxFrameRetries	/	3

It should be noted here that, each time the node draws a random backoff value, it has to make sure that it has enough time for transmitting the packet within the current CAP. If it has enough time to finish both the backoff and the transmission (including CCAs and ACK reception), it shall proceed as indicated before. Otherwise, if it can finish the backoff, but there is not enough time for completing the steps for transmission procedure, it shall defer the entire transmission by performing another backoff at the beginning of the next CAP and proceeding as usual. Finally, if there is not even enough time to finish the backoff procedure, it shall perform as many BPs of the backoff that fit in the current CAP, and then continue the remainder of the backoff in the next CAP.

1.3 Markov Chains for the Slotted CSMA/CA

In this section, we will briefly review the different Markov chain models available in the literature which model the behavior of the IEEE 802.15.4 MAC protocol. We will then focus in the next section on the model presented by Pollin et al. in [6], which is the model we will be using for the present work.

The behavior of the slotted CSMA/CA in an IEEE 802.15.4 network has been widely investigated in the literature using the same approach introduced by Bianchi [7] for the traditional IEEE 802.11 CSMA/CA. In all these works, the behavior of the network is analyzed through modeling a single node's behavior with a discrete-time Markov chain. The state of each node evolves through its corresponding Markov chain independently of other nodes' states except for when it is sensing the channel. As it was mentioned earlier, each node can attempt a transmission only after it has sensed the channel idle for two consecutive time slots (CCA_1 and CCA_2) after finishing its backoff. The probability that it senses the channel idle in these two time slots depends on whether other nodes are transmitting or not. In all the works discussed in this section, it is assumed that the probability of sensing the channel idle is independent of the backoff stage in which CCA_1 and CCA_2 are performed. We will base our model on the same assumption, but as we show in Section 1.6, these probabilities do depend on the backoff stage their corresponding CCA is performed in. We will also discuss the parameters that are most affected by this assumption.

To avoid any confusion, in the following discussion we will consistently refer to the probability of sensing the channel busy when performing CCA_1 and CCA_2 as α and β respectively, independently of the notation used in the discussed work. Since the CCA states are the only states in the Markov chain where the dependence of the nodes come into play, calculating α and β accurately is the key to the correct analysis of the network. For this reason, in discussing the prior work, we will be mostly focused on the way these probabilities are calculated as the main criteria for evaluating the accuracy of the models.

Mišić et al. in [8] propose a Markov chain model to analyze the slotted CSMA/CA under saturated and unsaturated traffic conditions in a beacon-enabled network in ACK mode.

The superframe structure and the retransmissions are not considered in their model. In [9], they extend the model of [8] in the unsaturated case, modeling also the superframe structure and retransmissions. For the saturated case in [8], they construct a per-node Markov chain. However, they only include one state for transmission, even though the transmission may take more than one BP. They also do not include the corresponding states for the time spent receiving and waiting for the ACK. Therefore, in the normalizing condition for the steady state probabilities of the chain, the BPs spent for transmission and ACK are not accounted for. Furthermore, even though when calculating α they do consider the ACK, they neglect its effect when calculating β. Finally, when calculating both α and β, they implicitly assume that the probability to start transmission is independent for all the nodes. But in fact, this probability is highly correlated for different nodes since before a transmission a node has to sense the channel idle for two BPs, and therefore, for two nodes to be transmitting simultaneously, they have to have sensed the channel exactly at the same time. Since in such a case both nodes observe the same channel state, the probability of two nodes transmitting at the same BP is highly dependent. For the unsaturated condition in both [8] and [9], they extend the Markov chain model of the saturated case, and therefore, all the aforementioned issues apply to these cases as well. In neither case the analytical results are validated with simulation.

It should be noted here that, in Bianchi's work on IEEE 802.11 in [7], the transmission states are also omitted from the chain. However, in that case this is justified and in fact necessary due to the structural difference between the IEEE 802.11 and the IEEE 802.15.4 CSMA/CA mechanisms. In IEEE 802.11, nodes are constantly sensing the channel while performing backoff, and freeze their backoff counter when there is a transmission on the channel. This implies that even though the backoff states in the Markov chain in [7] do not have a fixed duration, they all have the same *expected* duration. On the other hand, while a node is transmitting, its transmission is never interrupted and therefore, the transmission states cannot be included in the Markov chain model as they do not have the same expected duration as the backoff states. Thus, in Bianchi's model, all the states included in the chain have the same expected duration, and therefore, the steady state probabilities are well-defined. In IEEE 802.15.4, however, all transitions happen strictly at the boundaries of backoff periods and no sensing is done during the backoff. Instead, the sensing is done

only after the backoff during CCA_1 and CCA_2. This means that the backoff and sensing states all have the same fixed duration of exactly one BP. Therefore, representing the entire transmission (which lasts a fixed multiple of a BP) with only one state in the chain renders the steady state probabilities ill-defined, because when they are calculated, states with different duration are given the same weight.

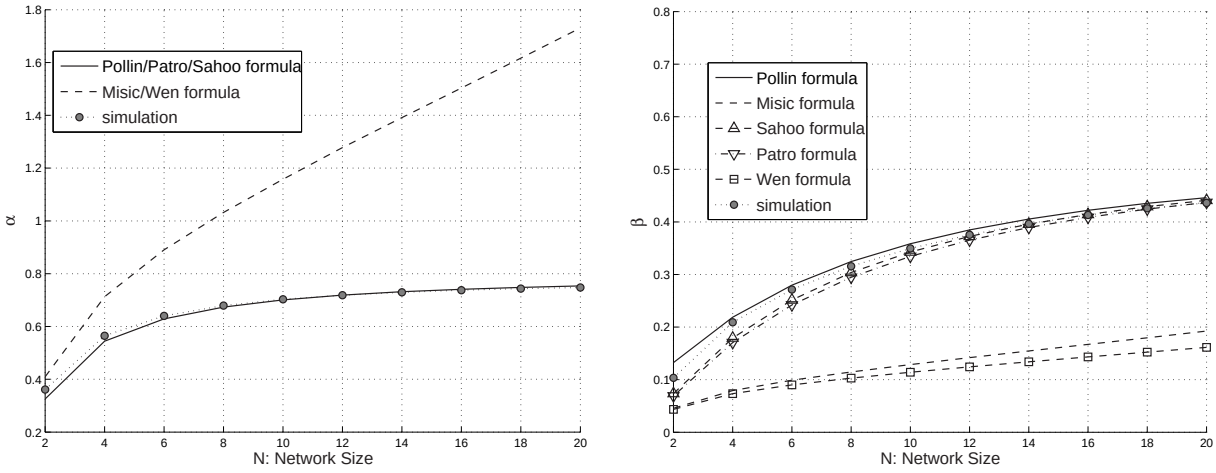

Figure 1.4: Comparison between the values of α and β obtained from formulas in [6] and [8]–[12], and the actual values obtained from simulation.

Pollin et al. in [6] suggest a simple but complete Markov chain model for the slotted CSMA/CA under saturated and unsaturated periodic traffic conditions in a beacon-enabled network in both ACK and no-ACK modes. They do not model the superframe structure. Unlike [8] and [9], their Markov chain includes a number of transmission states equal to the packet length (in the number of BPs). They base their model on the main assumption that the probability to start sensing the channel is independent across the nodes and properly consider the dependence between the nodes when calculating α and β. They validate their analytical results with simulations. However, as we will explain in more detail in Section 1.4.2 in their model a group of states are accounted for twice.

Other works using similar approaches to Pollin and Mišić include [10] and [11]. However, similar issues as the ones just mentioned can be observed in their models and calculations as well. For example, in [10] only one transmission state is included in the chain, and in [11] the same Markov chain model as in [6] is used where similarly a set of states are accounted for twice. Furthermore, when writing the normalizing condition for the chain they allow

the backoff exponent to increase above *macMaxBE*. The packet discard probability is not properly calculated either, as it does not include the cases where a packet fails the access procedure during a retransmission.

In more recent works, Wen et al. in [12] use a proper Markov chain model, but they do not consider the dependence in transmission probability of different nodes when calculating α and β. Finally, in [13], Jung et al. propose a new model based on the Mišić model in [9]. However, they too do not include all the transmission states in the Markov chain.

Figure 1.4 shows a comparison between the values of α and β obtained from the formulas in the aforementioned works and those obtained from simulation. Note that in all cases, we have plotted these parameters only for a network operating in no-ACK mode, with no retransmissions, no superframe structure, and under saturated traffic condition. We see that specially in the case of [8] and [12], the formulation for α and β offers an inacurate approximation to the actual values of these parameters. This, as we mentioned before, is due to the fact that they ignore the high dependence between the probabilities of starting transmission for different nodes. All discussed models, except [8], [9], and [12], use the same formulation for α. This is not the case for β, in which case, we note that Pollin et al's model offers the best estimate for most network sizes.

The IEEE 802.15.4 MAC features modelled in each of the works in [6] and [8]–[12] are summarized in Table 1.2.

Table 1.2: Prior Work Summary

Model includes	Pollin [6]	Misic [8]	Misic [9]	Sahoo [10]	Patro [11]	Wen [12]	Jung [13]
Saturated traffic	Yes	Yes	No	No	Yes	Yes	No
Unsaturated traffic	Yes	Yes	Yes	Yes	No	Yes	Yes
Retransmissions	No	No	Yes	Yes	Yes	No	Yes
Superframe structure	No	No	Yes	No	No	No	Yes
Correct # of TX states	Yes	No	No	No	Yes	Yes	No
Correct # of CCA states	No	Yes	Yes	Yes	No	Yes	Yes

1.4 System Model and Notation

In the present work, we will be using the Markov chain model presented by Pollin et al. in [6], with some modifications, and will be mostly following the notation thereof, with minor changes when necessary. Therefore, in this section, we will first describe this modified Markov chain model and its corresponding formulation, and will then compare it to the one presented in [6]. To validate our results, we will use simulations which reproduce the CSMA/CA mechanism in IEEE 802.15.4. More details about the simulation are to come in Section 1.5.

1.4.1 Markov Chain Model

In [6], the performances of a single hop LR-WPAN, made by N nodes and a PAN coordinator (i.e., the sink in a WSN) have been evaluated for uplink traffic. Both saturated and unsaturated periodic traffic conditions, and ACK and no-ACK modes have been considered. We have focused our attention on the saturated case (i.e., when each of the N nodes in the LR-WPAN, always has a packet available for transmission) in the no-ACK mode. The saturated case reflects a sensor network scenario in which an event is detected by many sensor nodes that want to transmit the gathered information, at the same time, to the sink node. We will not be considering the superframe structure in our model, i.e., we are assuming that the network is operating in a CAP with an infinite duration.

The behavior of a single node is modeled using a two-dimensional Markov chain, with states represented by $\{s(t), c(t)\}$ at a given backoff period t, as shown in Figure 1.5. Hereafter, we use the term time slot, or simply slot, to refer to a backoff period. All events happen at the beginning of a time slot. At a given time slot t, the stochastic process $s(t)$ represents the backoff stage when $s(t) \in \{0, \ldots, M\}$, and the transmission stage when $s(t) = -1$. When the node is in transmission (i.e., $s(t) = -1$), the stochastic process $c(t) \in \{0, \ldots, L-1\}$ represents the state of the transmission, i.e., the number of slots spent on the current transmission. L is the packet size, measured in the number of slots it takes for transmitting the packet, and includes the overhead introduced by the PHY and MAC

headers. When the node is in backoff, $c(t) \in \{0, \ldots, W_i - 1\}$ represents the value of the backoff counter, where $W_i = 2^{\min\{macMinBE+i, macMaxBE\}}$ is the size of the backoff window at backoff stage $s(t) = i \in \{0, \ldots, M\}$. Finally, when the node is performing one of the CCAs, $c(t)$ represents the value of the CCA counter, with $c(t) = 0$ during CCA_1 and $c(t) = -1$ during CCA_2. Note that the state $\{s(t), c(t)\} = \{i, 0\}$, has to be seen as a CCA_1 state and not as a backoff state as in [6]. In fact, although the randomly picked backoff window size at stage i can take any value in the set $\{0, \ldots, W_i - 1\}$, the value zero indicates no waiting and immediate sensing. In other words, if the backoff counter of a node is equal to zero, it immediately starts sensing the channel (i.e., it performs CCA_1).

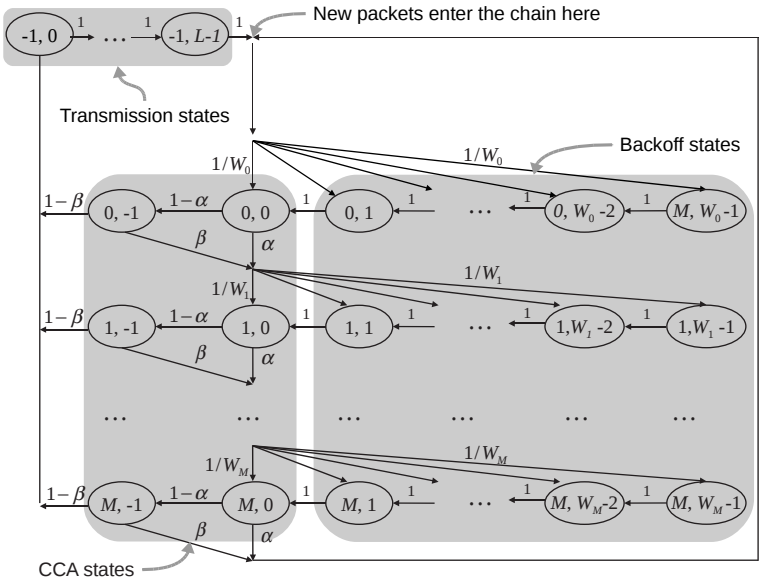

Figure 1.5: Markov Model for slotted CSMA/CA.

The parameter α in Figure 1.5 is the probability of assessing the channel busy during CCA_1, and β is the probability of assessing it busy during CCA_2, given that it was idle in CCA_1. In reality, the values of α and β for a given node depend not only on the backoff stage of that node, but also on that of other nodes in the system. However, for simplicity, we ignore this dependence and assume that the values of both α and β are the same for different backoff stages and are also independent of the backoff stage of other nodes. This assumption is used in all the prior work discussed in Section 1.3 and it is what allows us to model the network by only analyzing the individual Markov chain of a node in the network as shown in Figure 1.5. We will further scrutinize this assumption in Section 1.6. As it was

mentioned earlier, in this per-node Markov chain model, the effect of other nodes on the behavior of a given node is captured only through the values of α and β, and therefore, these two parameters play a key role in the model.

Let $b_{i,k}$ be the steady state probability of being in state $\{i,k\}$, i.e., $b_{i,k} = \lim_{t\to\infty} P\{s(t) = i, c(t) = k\}$. These steady-state probabilities are related to one another through the following equations:

$$b_{i,k} = \frac{W_i - k}{W_i} b_{i,0} \qquad 0 \le i \le M, 0 \le k \le W_i - 1 \tag{1.3}$$

$$b_{i,0} = (1-y)^i b_{0,0} \qquad 1 \le i \le M \tag{1.4}$$

$$b_{i,-1} = (1-\alpha) b_{i,0} \qquad 0 \le i \le M \tag{1.5}$$

$$b_{-1,k} = y \sum_{j=0}^{M} b_{j,0} = y\phi \qquad 0 \le k \le L-1 \tag{1.6}$$

where $y = (1-\alpha)(1-\beta)$, and ϕ is the probability that a randomly picked slot is spent performing CCA_1 which is given by

$$\phi = \sum_{j=0}^{M} b_{j,0} = \frac{1-(1-y)^{M+1}}{y} b_{0,0}. \tag{1.7}$$

By determining the interactions between the N nodes on the medium, the expressions for probabilities α and β have been derived in [6]. In short, the probability α, of finding channel busy during the first CCA is given by

$$\alpha = L\left[1-(1-\phi)^{N-1}\right] y. \tag{1.8}$$

In turn, β, the probability that there is a transmission in the medium when the considered node does its second sensing, is given by

$$\beta = \frac{1-(1-\phi)^N}{2-(1-\phi)^N}. \tag{1.9}$$

The values of ϕ, α and β can be determined by imposing the following normalizing condition:

$$\sum_{i=0}^{M}\sum_{k=0}^{W_i-1} b_{i,k} + \sum_{i=0}^{M} b_{i,-1} + \sum_{k=0}^{L-1} b_{-1,k} = 1 \tag{1.10}$$

which can be equivalently written as

$$\frac{b_{0,0}}{2}\left\{[3-2\alpha+2yL]\,\frac{1-(1-y)^{M+1}}{y} + 2^d W_0 \frac{(1-y)^{d+1}-(1-y)^{M+1}}{y} + W_0\frac{1-(2-2y)^{d+1}}{2y-1}\right\} = 1 \tag{1.11}$$

where $W_0 = 2^{macMinBE}$ and $d = macMaxBE - macMinBE$.

As can be seen in Figure 1.6, (1.8) and (1.9) offer a good approximation to the values of α and β for large network sizes. But for example at $N = 2$, the formulas introduce about 10% and 30% approximation errors for α and β, respectively. As we will see in the next sections, the impact of this error can be negligible when calculating some parameters of the network, but for certain parameters, it has a noticeable negative impact.

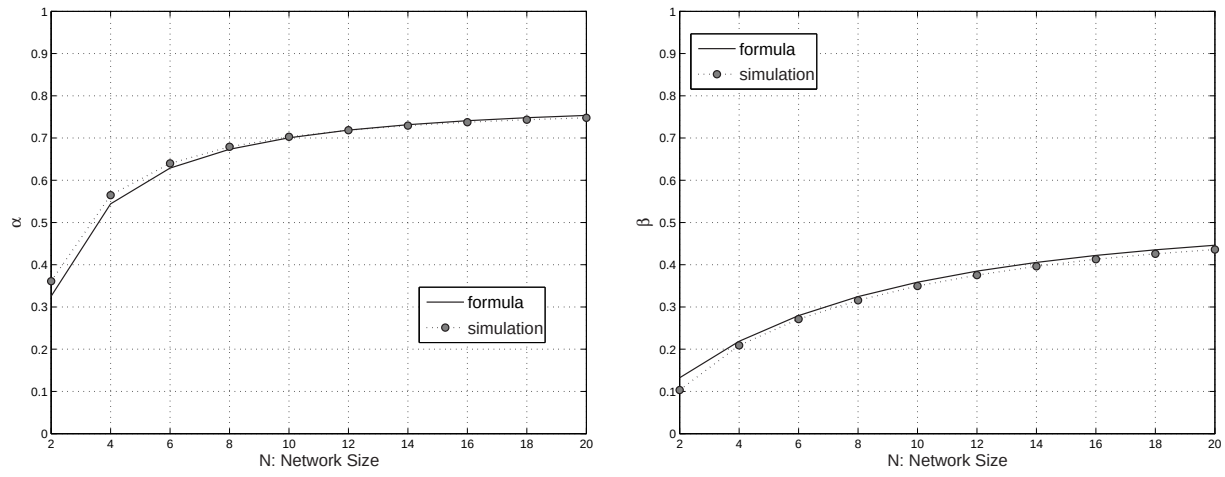

Figure 1.6: Comparison between the values of α and β obtained from (1.8) and (1.9), and those obtained from simulation.

1.4.2 Discussion of the Pollin Model

As was mentioned earlier, the model described in the previous section closely follows that of Pollin model. However, there were some necessary modifications made to that model which we list here.

The main assumptions: The main assumptions that enable us to use the described Markov chain model are the following:

A1. The probability to start sensing the channel, ϕ, is independent across nodes;

A2. The probability to sense the channel busy during CCA_1 and CCA_2 does not depend on the backoff stage where the corresponding CCA is performed. In other words, $\alpha_i = \alpha$ and $\beta_i = \beta$ for $i \in \{0, \ldots, M\}$;

A3. The probability that a node is in a given backoff stage, is independent of that of other nodes;

A4. The probability of sensing the channel busy during a CCA does not depend on the random backoff value drawn in the backoff stage preceding the CCA.

In [6], A1 is the only stated assumption. In what follows, specially in Section 1.6, we will discuss the significance of these assumptions .

The normalizing condition of the Markov chain steady state probabilities: In [6] the following equation is given as the normalizing condition for the steady state probabilities:

$$\sum_{i=0}^{M} \sum_{k=0}^{W_i-1} b_{i,k} + \sum_{i=0}^{M} b_{i,-1} + \sum_{i=0}^{M} b_{i,-2} + \sum_{k=0}^{L-1} b_{-1,k} = 1 \tag{1.12}$$

where $b_{i,-1}$ and $b_{i,-2}$ in their notation correspond to the first and second CCA, respectively. On the other hand, states $b_{i,0}$ also correspond to the first CCA, because, as we mentioned earlier, when the backoff counter reaches zero, the node will immediately start sensing. Even though the Markov chain depicted in [6] does not contain any state $b_{i,0}$, in the above normalizing condition, both of the states $b_{i,0}$ and $b_{i,-1}$ are counted and therefore, the states $b_{i,0}$, as per our notation, are counted twice. This normalizing condition together with (1.7), (1.8), and (1.9) constitute a system of equations that is used in [6] to numerically obtain α,

β, and ϕ. Therefore, the aforementioned overcount in the normalizing condition affects the values obtained for these variables.

1.5 Results

In this section, we use the Markov chain model to calculate different important parameters of the system, such as delay, energy consumption, throughput and efficiency.

In order to validate the analytical results, we simulate the behavior of the slotted CSMA/CA using an event-driven simulator written in Matlab. We reproduce the network under the same conditions of the analytical model, i.e., we analyze the channel access mechanism in the no-ACK mode, and disregarding the superframe structure. It should be noted that for the simulation we do not make any assumption on the dependence of the nodes or backoff stages, and therefore, the simulation truly reflects the behavior of the network under the aforementioned conditions, and not the behavior of the Markov chain model.

In what follows, all the parameters have been defined as functions of α, β and ϕ. In [6], ϕ is calculated by numerically solving their corresponding (1.8) – (1.10). In our work, when plotting the curves from the analytical formulation to validate their accuracy, we use the value of ϕ found by simulation, and then calculate α, β, and the rest of the parameters from ϕ. These curves are indicated in the figures' legends by "formula".

For the MAC parameters, we use the default values defined by the standard (see Table 1.1) and fix the packet length for all nodes to $L = 7$ time slots. The simulation is run for a duration of $T = 10^8$ slots.

1.5.1 Average Delay

In the no-ACK mode, the average delay for a successfully transmitted packet, i.e., the number of slots it takes from the moment it reaches the head of the line to the moment it arrives at its destination, is given by

$$\bar{D} = \bar{n}_{B_{suc}} + \bar{n}_{C_{suc}} + L \tag{1.13}$$

where $\bar{n}_{B_{suc}}$ and $\bar{n}_{C_{suc}}$ are the mean number of slots spent performing backoff and CCA, respectively, before a successful transmission. The average delay calculated above, can be equivalently viewed as the packet service time in a saturated IEEE 802.15.4 network of queues.

Note that based on assumptions A2 and A3, the number of slots spent in backoff or CCA before transmission for packets that are successfully transmitted and those that end up having a collision should be the same, i.e., $\bar{n}_{B_{suc}} = \bar{n}_{B_{col}} = \bar{n}_{B_{tx}}$ and $\bar{n}_{C_{suc}} = \bar{n}_{C_{col}} = \bar{n}_{C_{tx}}$. For this reason, in Section 1.5.3, we obtain the expressions for the values of $\bar{n}_{B_{tx}}$ and $\bar{n}_{C_{tx}}$, which we use to calculate the delay as described above.

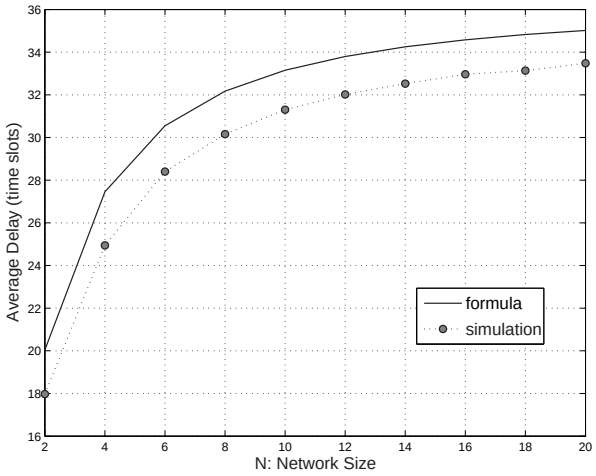

Figure 1.7: Comparison between formula and simulation values for $\bar{D}$.

As can be seen in Figure 1.7, the value of delay calculated from (1.13) and that obtained from simulation have a constant difference of about two slots for all values of network size N. This difference is due to assumption A2. A similar difference is observed in the values of $\bar{n}_{B_{tx}}$ and $\bar{n}_{C_{tx}}$ as we will see in Section 1.5.3, where we will discuss this issue in more detail.

1.5.2 Average Power Consumption

For every packet that is transmitted or discarded, the node uses different power levels depending on whether it is in backoff, sensing, or transmission. Therefore, the average power

consumption per node (in joules/s) is given by

$$\bar{P} = \frac{\bar{n}_{_B} W_{id} + \bar{n}_{_C} W_{rx} + L(1-p_f) W_{tx}}{\bar{n}_{_B} + \bar{n}_{_C} + L(1-p_f)} \tag{1.14}$$

where $\bar{n}_{_B}$ and $\bar{n}_{_C}$ are the average number of slots spent in backoff and CCA, respectively. These parameters are derived in Section 1.5.3. In turn, p_f is the packet discard probability due to access procedure failure, and it is given by

$$p_f = (1-y)^{M+1}. \tag{1.15}$$

The power consumed by the radio transceiver in mode x, is given by $W_x = I_x \times V_{DD}$. Here, I_x is the amount of current consumption for operating mode x, and V_{DD} is the supply voltage. For illustrative purposes, we use the parameter values specified for Chipcon 802.15.4-compliant RF transceiver CC2430 [14]. The CC2430 provides four different power modes, PM0 to PM3. PM0-TX and PM0-RX are used for transmission and reception modes, respectively and we have supposed that the device uses PM2 as idle mode. The current consumptions of CC2430 power modes and the supply voltage, V_{DD}, are given in Table 1.3.

Table 1.3: CC2430 Specifications

Parameter	Value	Unit	Power Mode
I_{tx}	26.9	mA	PM0-TX
I_{rx}	26.7	mA	PM0-RX
I_{id}	0.5	μA	PM2
V_{DD}	3	V	–

As can be seen in Figure 1.8, the value for the average power obtained from (1.14) matches well its value from simulation. We see here that the average power consumption per single node decreases with larger N. This is because the packet discard probability, p_f, increases with N and therefore, each node is able to transmit fewer packets as the network size grows. As most of the power consumption happens during the actual transmission of the packet, this means that on average less power is consumed.

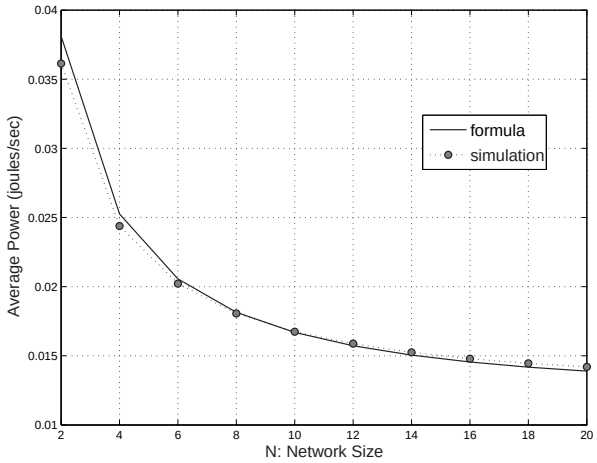

Figure 1.8: Comparison between formula and simulation values for $\bar{P}$.

1.5.3 Mean Number of Backoffs and CCAs

As we saw earlier, in order to calculate the average delay and the average power consumption, we need to know how many slots on average a node spends performing backoff and CCA before transmitting or discarding every packet. In this section, we will derive these parameters using the Markov chain model described earlier.

Mean Number of Backoffs

The average number of backoffs a transmitted packet goes through, $\bar{n}_{B_{tx}}$, is different from that of a discarded packet, $\bar{n}_{B_f}$. This is because a discarded packet always goes through all the backoff stages of the chain before exiting it, whereas a transmitted packet might exit the chain from any backoff stage.

The mean number of slots spent in backoff stage i, every time it is entered, is given by $(W_i - 1)/2$. This is because the backoff value is drawn according to a discrete uniform distribution in $[0, W_i - 1]$. Therefore, $\bar{n}_{B_{tx}}$, the mean number of backoffs before transmission, is given by

$$\bar{n}_{B_{tx}} = \sum_{i=0}^{M} \left(\sum_{k=0}^{i} \frac{W_k - 1}{2} \right) \frac{p_{S_i}}{1 - p_f} \tag{1.16}$$

where p_{S_i} is the probability that the channel access procedure ends successfully (i.e., the packet is sent) in backoff stage i and it is given by

$$p_{S_i} = y(1-y)^i \ , \qquad 0 \leq i \leq M. \tag{1.17}$$

After a bit of algebra, we obtain

$$\begin{aligned}\bar{n}_{B_{tx}} = \frac{1}{1-p_f} \Bigg\{ & W_0 y \frac{1-(2-2y)^{d+1}}{2y-1} - \frac{1-y}{2y} - \frac{W_0+1}{2} + 2^{d-1} W_0 \left(3 + \frac{1-y}{y}\right)(1-y)^{d+1} \\ & - \left[W_0 2^{d-1}(1-d) - \frac{W_0+1}{2} + \left(\frac{W_0 2^d - 1}{2}\right)\left(\frac{1-y}{y}\right)\right](1-y)^{M+1} \Bigg\}. \end{aligned} \tag{1.18}$$

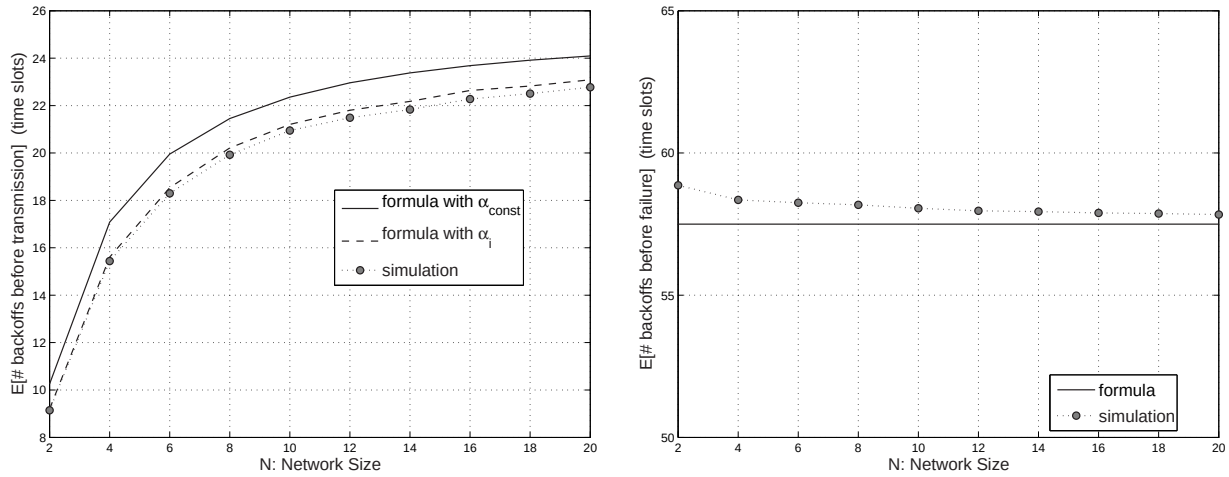

(a) $\bar{n}_{B_{tx}}$ from simulation compared to its value from formula applied to the constant α, and to α_i.

(b) $\bar{n}_{B_f}$ from simulation and formula applied to constant α.

Figure 1.9: Comparison between formulas and simulation values for $\bar{n}_{B_{tx}}$ and $\bar{n}_{B_f}$.

Figure 1.9(a) shows the value of $\bar{n}_{B_{tx}}$ obtained from (1.16) and that obtained from simulation. As we see here, there is an almost constant difference of less than two slots between the analytical and simulation results. This is again due to assumption A2. For this reason, in the same figure we have also plotted the value of $\bar{n}_{B_{tx}}$ calculated using the actual values of α_i and β_i for every backoff stage i obtained from simulation. In this case, the value of

$\bar{n}_{B_{tx}}$ is still given by (1.16), but p_{S_i} has to be calculated using the following expression

$$p_{S_i} = \begin{cases} y_0, & i = 0, \\ y_i \prod_{k=0}^{i-1} (1 - y_k), & 1 \leq i \leq M \end{cases} \tag{1.19}$$

where $y_i = (1 - \alpha_i)(1 - \beta_i)$. Also, the probability p_f has to be calculated as follows

$$p_f = \prod_{k=0}^{M} (1 - y_k). \tag{1.20}$$

In turn, a packet is discarded when the node goes through every backoff stage in the chain and fails to access the channel in all the $M + 1$ consecutive backoff stages. Therefore, $\bar{n}_{B_f}$, the mean number of slots spent in backoff before an access procedure failure, is given by

$$\bar{n}_{B_f} = \sum_{k=0}^{M} \left(\frac{W_k - 1}{2} \right) \frac{p_{S_M}}{p_f} = \sum_{k=0}^{M} \frac{W_k - 1}{2} = W_0 2^d \left(1 + \frac{M - d}{2} \right) - \frac{W_0 + M + 1}{2}. \tag{1.21}$$

As seen in (1.21), $\bar{n}_{B_f}$ is not a function of α and β and therefore, the expression is valid independently of assumption A2. Moreover, $\bar{n}_{B_f}$ is not a function of N, because every discarded packet goes through all the backoff stages, and hence, the number of slots spent in backoff for a discarded packet only depends on the random backoff value drawn at every backoff stage. Assuming A4, for a given backoff stage i, an average of $(W_i - 1)/2$ slots are spent in backoff before performing the CCA. Figure 1.9(b) shows the value of $\bar{n}_{B_f}$ from simulation and formula. We see here that the value obtained from (1.21) is very close but always slightly lower than the one obtained from simulation. This is because α is not completely independent of the random backoff value drawn. In fact, the packets that end up being discarded are those that are less "fortunate" and draw a larger backoff value.

Finally, for a generic packet, the mean number of slots that a node spends in backoff before transmitting or discarding the packet, is given by

$$\bar{n}_B = \bar{n}_{B_{tx}} (1 - p_f) + \bar{n}_{B_f} p_f. \tag{1.22}$$

Mean Number of CCAs

For a packet to be transmitted, a node needs to succeed in the access procedure in some backoff stage. If the access procedure succeeds in stage i, it means that it had two successful CCAs in that stage, and at least one failed CCA in stages 0 to $i-1$. In other words, it must have had k successful CCA_1's and failed CCA_2's, for some $k \leq i$, and $i-k$ failed CCA_1's. This event happens with probability

$$p_{f_{i,k}} = \binom{i}{k} [(1-\alpha)\beta]^k \cdot \alpha^{i-k}. \tag{1.23}$$

In this case, there will be a total of $i+k$ CCAs performed during the failed accesses plus an additional two successful CCAs at stage i where the access procedure succeeds. Thus, considering that the successful access at stage i happens with probability y, the mean number of CCAs before a successful access procedure is given by

$$\begin{aligned} \bar{n}_{C_{tx}} &= y \sum_{i=0}^{M} \sum_{k=0}^{i} (i+k+2) \frac{p_{f_{i,k}}}{1-p_f} \\ &= 2 + [2(1-y) - \alpha] \left[\frac{1}{y} - (M+1) \frac{(1-y)^M}{1-p_f} \right]. \end{aligned} \tag{1.24}$$

In the case of an access procedure failure, there are $M+1$ failed attempts and no successful consecutive CCAs. Therefore, the mean number of CCAs due to an access failure is given by

$$\bar{n}_{C_f} = \sum_{k=0}^{M+1} (M+1+k) \frac{p_{f_{M+1,k}}}{p_f} = (M+1) \left(2 - \frac{\alpha}{1-y} \right). \tag{1.25}$$

Figure 1.10(a), shows the value of $\bar{n}_{C_{tx}}$ obtained from (1.24) and from simulation. As in the case of $\bar{n}_{B_{tx}}$, we see here that there is a difference (although smaller) between simulation and formula. We conjecture that this difference is also due to assumption A2. However, we will not validate this conjecture here, since calculating $\bar{n}_{C_{tx}}$ as a function of α_i and β_i is a lot more complicated than calculating it for a constant α and β. This is because to calculate $\bar{n}_{C_{tx}}$ as a function of α_i and β_i, we have to consider each different possible success sequence separately. In other words, when we assume that α and β are constant, we only need to

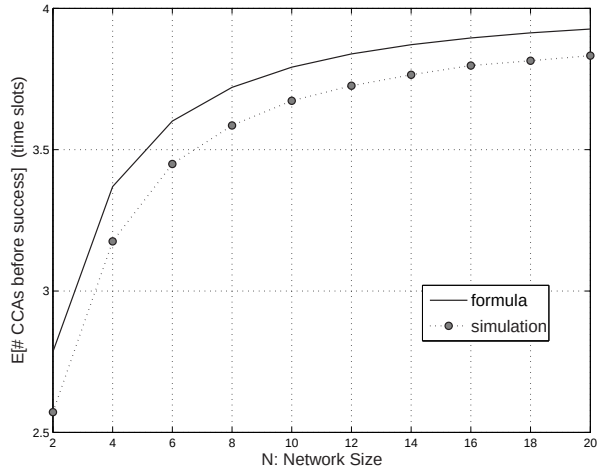

(a) $\bar{n}_{C_{tx}}$ from simulation and formula.

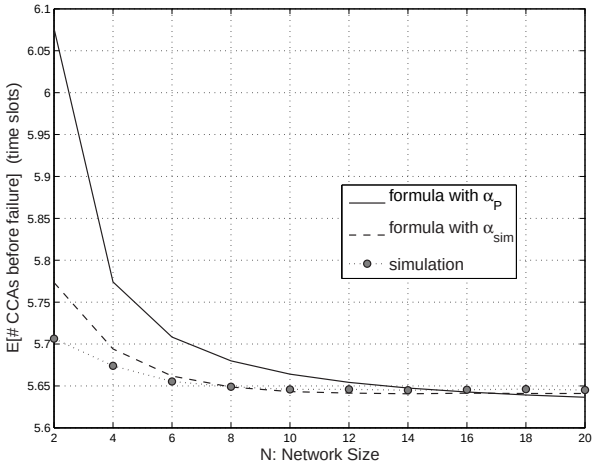

(b) $\bar{n}_{C_f}$ from simulation compared to its value obtained from formula applied to α_P (α calculated from formula proposed by Pollin et. al), and to α_{sim} (α from simulation).

Figure 1.10: Comparison between formula and simulation values for $\bar{n}_{C_{tx}}$ and $\bar{n}_{C_f}$.

consider the number of CCA_1's and CCA_2's performed before a transmission. But when α and β are a function of the backoff stage, we also need to consider what exactly happens in each backoff stage for all possible cases.

The value of $\bar{n}_{C_f}$ obtained from analysis and simulation is compared in Figure 1.10(b). In this figure, we have plotted two different curves for the value of $\bar{n}_{C_f}$ from formula. Indicated by "formula with α_P" is what we have been thus far indicating by only "formula", and it is basically found by applying (1.25) to α and β as derived from (1.8) and (1.9). Instead, the curve indicated by "formula with α_{sim}" is plotted by applying the same equation to the value of α and β directly obtained from simulation. We see that in the latter case, we get significantly better results. This means that the difference between the simulation and formula is not due to any inaccuracy in (1.25), but due to the inaccuracy in calculating α and β using (1.8) and (1.9) for small values of N. This inaccuracy was also evidenced in Figure 1.6.

Finally, the mean number of CCAs for a generic packet is given by

$$\bar{n}_C = \bar{n}_{C_{tx}}(1 - p_f) + \bar{n}_{C_f} p_f. \tag{1.26}$$

1.5.4 Efficiency

We define the efficiency, η, as the ratio between the per-node troughput and the power consumption, in bits/joule, that is given by

$$\eta = \frac{A \times S}{P}. \tag{1.27}$$

Here P is the average power consumption given by (1.14); S is the per-node throughput, defined as in [6] as the proportion of time that a node spends in successful transmission, given by $S = Ly\phi(1-\phi)^{N-1}$; and finally, A is a constant to convert the throughput to bits/s and is given by $A = B_{bp}/t_{bp}$, where $B_{bp} = 80$ is the number of bits transmitted in one backoff period, and $t_{bp} = 0.32$ ms is the duration of a backoff period.

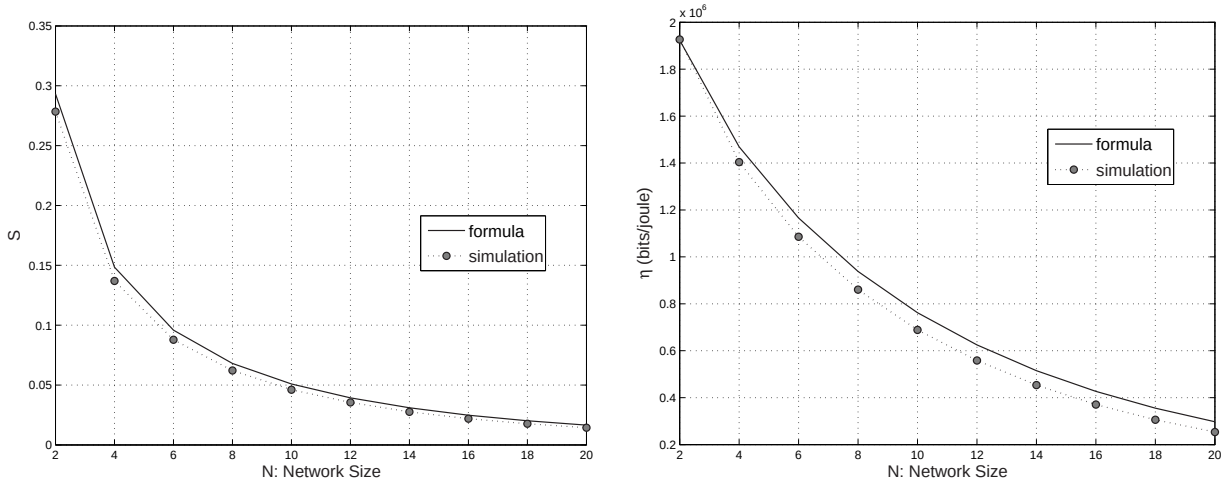

(a) Per-node throughput

(b) Efficiency

Figure 1.11: Comparison between formula and simulation values for throughput and efficiency.

Figure 1.11 shows the comparison between simulation and analysis for both throughput, S, and efficiency, η. As we can see in both cases, the analytical formulas offer a good approximation to the actual value of the corresponding parameter.

1.6 Analysis of the Model Assumptions

1.6.1 Dependence of α and β on the Backoff Stage

As was mentioned earlier, in the Markov chain model of Figure 1.5, it was assumed for simplicity that the probability of sensing the channel busy during CCA_1 and CCA_2 at a given time t was independent of the backoff stage the node is in (assumption A2). This allowed us to use a constant value for both α and β for all backoff stages, which in turn greatly simplified the derivations and analysis which followed. But as we saw in the previous section, when calculating the value of certain parameters, such as $\bar{n}_{B_{tx}}$, $\bar{n}_{C_{tx}}$, and therefore the average delay $\bar{D}$; this assumption does not result in a very good approximation of those parameters.

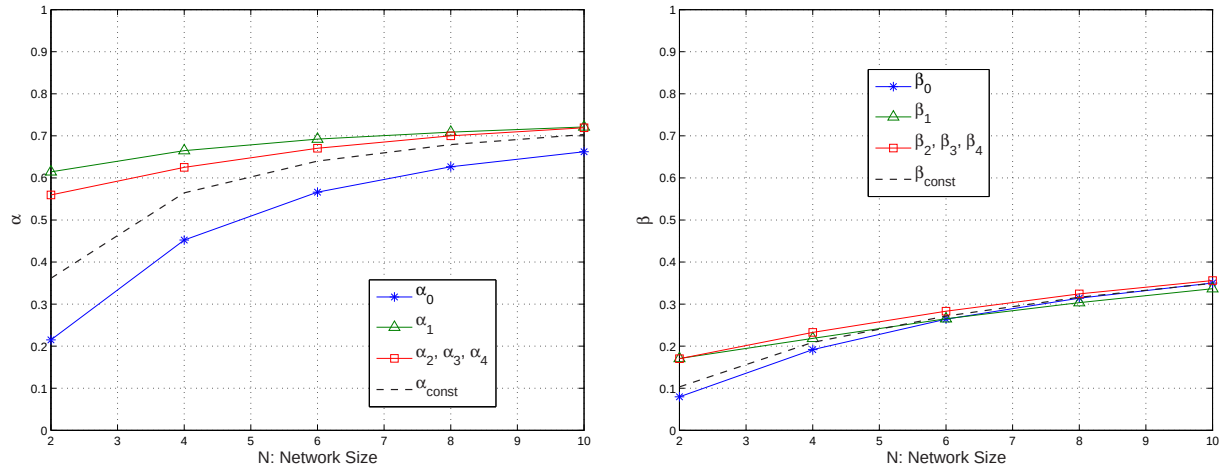

(a) α for different backoff stages

(b) β for different backoff stages

Figure 1.12: Dependence of α and β on the backoff stage.

Figure 1.12 shows the values of α_i and β_i for each backoff stage i. As we see here, α is in fact very dependent on the backoff stage. This difference is particularly noticeable between the first backoff stage ($i = 0$) and the rest of the backoff stages. This can be explained by observing that a node that is in the first backoff stage on average draws a smaller backoff value than other nodes that are competing with it. Additionally, the joint probability of two nodes being in the first backoff stage is particularly small (as we will see in Section 1.6.2).

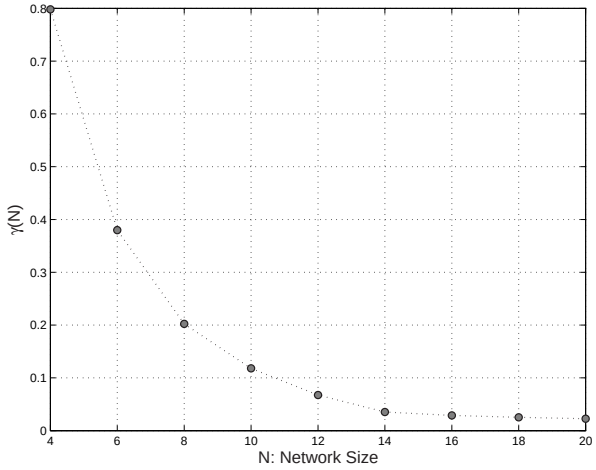

Figure 1.13: Dependence metric, $\gamma(N)$.

This means that a node that is in the first backoff stage is given an opportunity with not much competition compared to when it is in any other stage. Therefore, it is very likely for it to find the channel idle. We further see that most of this dependence is absorbed by the first CCA as when it comes to β, different backoff stages experience a very similar probability of finding the channel busy.

1.6.2 Dependence of the Backoff Stage of a Node on That of Other Nodes

Figure 1.13 shows the dependence of the backoff stage of a node on that of other nodes. The dependence metric $\gamma(N)$ is defined as the maximum relative difference between the joint probability and the product of the marginal probabilities of two nodes N_1 and N_2 being in backoff stages i and j respectively, when there are N nodes in the network. In other words,

$$\gamma(N) = \max_{i,j} \left\{ \frac{f_{S_1,S_2|N}(i,j) - f_{S_1|N}(i) f_{S_2|N}(j)}{f_{S_1,S_2|N}(i,j)} \right\} \tag{1.28}$$

where S_i is the random variable indicating the backoff stage of node i at a randomly chosen time slot in the steady state, and $f_X(x)$ indicates the probability mass function (pmf) of the random variable X at a given point x.

As we see in Figure 1.13, for small number of nodes, there is a strong dependence be-

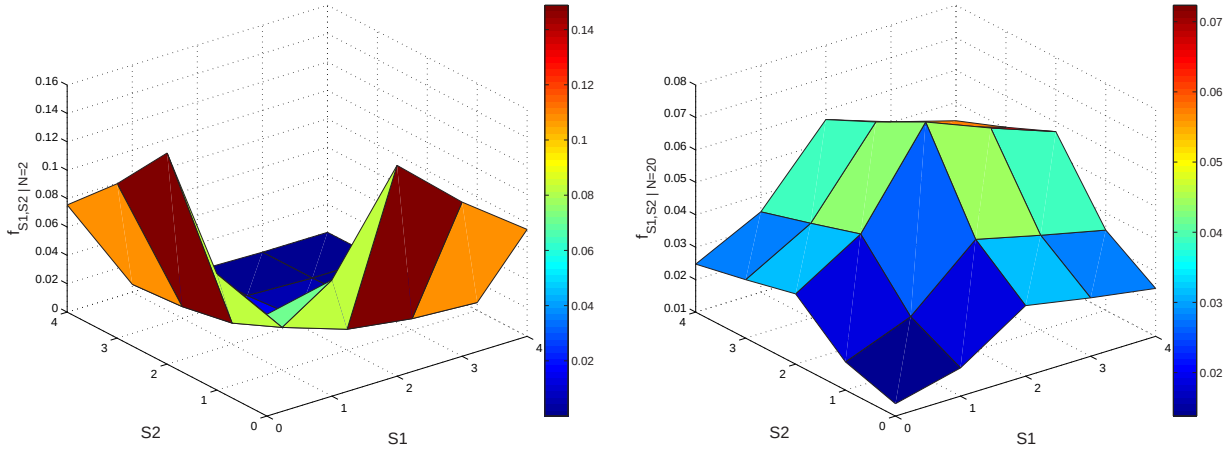

(a) N = 2 (b) N = 20

Figure 1.14: Joint pmf of the backoff stages of two nodes $f_{S_1,S_2|N}(i,j)$.

tween the backoff stages of different nodes. However, as the network grows, this dependence becomes less and less noticeable.

Figure 1.14(a) shows the joint pmf for the backoff stages of two nodes for the two cases of $N = 2$ and $N = 20$. We see that for $N = 2$, with high probability, at least one node is in the first backoff stage, while the other is in one of the other backoff stages. In this case, the probability of both nodes being in higher backoff stages simultaneously is extremely small. This indicates a high chance of successful transmission for $N = 2$ (and in general for small numbers of nodes). The situation is quite different in a network with a larger number of nodes. We see in Figure 1.14(b) that for $N = 20$, the nodes spend more time in the higher backoff stages of the chain, indicating a greater chance of failure. However, we observe that in both cases, even though the probability of a node being in the first backoff stage is not small (each packet has to go through the first backoff stage once in its lifetime irrespective of the value of N), the joint probability of two nodes being in the first backoff stage is relatively very small. As we mentioned earlier, this explains why α_0 is different from α_i for $i > 0$.

1.7 Conclusion and Outlook

ZigBee, with IEEE 802.15.4 as its link and access technology, will undoubtedly play a central part in the growth of the Internet of Things (IoT), the wireless, and heterogeneous extension of the wireline Internet. This can not only be attributed to its large international support by major vendors but also to its sufficiently good performance. This performance behavior has been the focus of this chapter, where we concentrated solely on the MAC assuming PHY and networking protocols given.

After having reviewed key parameters contributing to the MACs performance behavior and prior publications in this field, we have moved on to its characterization and then analysis. We have exposed the correct mathematical formulation of the throughput, delay and energy efficiency behavior as a function of the number of contenting nodes, the packet length, the depth of the backoff stage, etc. This formulation can then be used to tune the system parameters in order to optimize a given metric, e.g., efficiency.

In the process of developing the aforementioned formulation, we have also been able to pinpoint the reasons why the results obtained from event simulations sometimes differ from those gathered from a Markov-chain-based analysis. This identifies the limitations of this popular approach, thereby facilitating its adequate utilization.

At the same time, several important issues have not been touched upon, be it because no analytical expressions are available yet or due to space limit. Far from being exhaustive, some of these are summarized below and subsequently discussed in greater details:

- impact of finite buffer lengths;
- non-saturated traffic conditions;
- impact of capture effect due to shadowing;
- relayed traffic in more complicated topologies;
- parametric mapping to known WSN MAC families;
- extension to emerging IEEE 802.15.4e, .15.4g and .15.4f MACs.

Finite buffers lead to buffer overflows and hence to additional packet losses which have so far not been catered for. These losses are non-linear functions of the packet arrival rate and

the buffer length. To include this in the current analysis, some additional transitions need to be introduced into the Markov state diagram.

Current analysis only caters for saturated traffic conditions, i.e. every node has always a packet to transmit. To extend the analysis rigorously to any possible traffic arrival conditions, additional states and transitions need to be introduced. However, some simplifying heuristics can be invoked using a binomial expansion of active nodes and the results of the above exposed theory.

Capture is referred to the effect when a node can receive a packet even though more than one transmission happens simultaneously. This is facilitated by shadowing at link level where an ongoing transmission is not perturbed simply because the receiver is shadowed by larger objects from any other ongoing transmission. A rigorous analysis of the capture effect is quite involved but, again, involving some simplifying heuristics may help finding a suitable solution.

Relayed traffic is — in a sense — redundant traffic since it involves the re-transmission of already received information. It clearly impacts end-to-end delay and throughput, as well as the systems energy efficiency. Relayed packets are also usually treated differently from newly generated packets. All this is currently not reflected in the analysis where a rigorous approach is again seen to be prohibitively complex.

As already alluded to in the introduction, MACs for WSNs typically follow the following taxonomy: framed MACs for delay-constrained high traffic loads; contention-based MACs with common active periods for medium traffic loads; duty-cycled sampling protocols for low traffic loads; and hybrids thereof [4]. These have proved to be optimum under respective traffic conditions. A formal derivation of IEEE 802.15.4 MAC parameters realizing these MACs is still an open problem and certainly worth investigating.

Finally, novel MAC families are emerging at the time of the writing of this book. These are mainly the IEEE 802.15.4e, .15.4g and .15.4f MACs, where the first is for delay-constrained embedded system solutions, the second for active RFID systems, and the last for smart utility networks. Applying the derived analysis and synthesis to these emerging standards

is an open issue deserving attention.

References

[1] IEEE std. 802.15.4. *Part. 15.4: Wireless Medium Access Control (MAC) and Physical Layer (PHY) Specifications for Low-Rate Wireless Personal Area Networks (LR-WPANs)*. IEEE standard for Information Technology, IEEE-SA Standards Board, Sept. 2006.

[2] IETF WG. IPv6 over Low power Wireless Personal Area Networks. Available online: http://tools.ietf.org/wg/6lowpan/.

[3] IETF WG. Routing Over Low Power and Lossy Networks. Available online: http://tools.ietf.org/wg/roll/.

[4] A. Bachir, M. Dohler, T. Watteyne, and K.K. Leung. MAC Essentials for Wireless Sensor Networks. *IEEE Communications Surveys and Tutorials*, to appear.

[5] IEEE std. 802.11. *Information Technology - Telecommun. and Information Exchange between Systems. Local and Metropolitan Area Networks. Specific Requirements. Part 11: Wireless LAN MAC and PHY Specifications.* ANSI/IEEE Std. 802.11, ISO/IEC 8802-11, 1st edition, 1999.

[6] S. Pollin, M. Ergen, S. C. Ergen, B. Bougard, L. Van der Perre, I. Moermann, A. Bahai, P. Varaiya, and F. Catthoor. Performance Analysis of Slotted Carrier Sense IEEE 802.15.4 Medium Access Layer. *IEEE Transactions on Wireless Communications*, 7(9), Sept. 2008.

[7] G. Bianchi. Performance Analysis of the IEEE 802.11 Distributed Cooridination Function. *IEEE Journal on Selected Areas in Communications*, 18(3):535–547, 2000.

[8] J. Mišić, S. Shafi, and V. B. Mišić. The Impact of MAC Parameters on the Performance of 802.15.4 PAN. *Ad Hoc Networks*, 3(5):509–528, Sept. 2005.

[9] J. Mišić and V. B. Mišić. Access Delay for Nodes with Finite Buffers in IEEE 802.15.4 Beacon Enabled PAN with Uplink Transmissions. *Computer Communications*, 28(10), Jun. 2005.

[10] P.K. Sahoo and J. Sheu. Modeling IEEE 802.15.4 based Wireless Sensor Network with packet retry limits. In *Proc. of the 5th ACM Symposium on Performance Evaluation of*

Wireless Ad Hoc, Sensor, and Ubiquitous Networks, Canada, Oct. 2008.

[11] R. K. Patro, M. Raina, V. Ganapathy, M. Shamaiah, and C. Thejaswi. Analysis and improvement of contention access protocol in IEEE 802.15.4 star network. In *Proc of IEEE Internatonal Conference on Mobile Adhoc and Sensor Systems (MASS'07)*, 2007.

[12] H. Wen, C. Lin, Z.J. Chen, H. Yin, T. He, and E. Dutkiewicz. An Improved Markov Model for IEEE 802.15. 4 Slotted CSMA/CA Mechanism. *Journal of Computer Science and Technology*, 24(3):495–504, 2009.

[13] C.Y. Jung, H.Y.Hwang, D.K.Sung, and G.U.Hwang. Enhanced Markov Chain Model and Throughput Analysis of the Slotted CSMA/CA for IEEE 802.15.4 Under Unsaturated Traffic Conditions. *IEEE Transactions on Vehicular Technology*, 58(1), Jan. 2009.

[14] Chipcon Products from Texas Instruments. *CC2430 Preliminary Data Sheet (rev. 2.1) SWRS036F*, Jun. 2007.